

ORIGINAL ARTICLE

Strong molecular weight effects of gate-insulating memory polymers in low-voltage organic nonvolatile memory transistors with outstanding retention characteristics

Jooyeok Seo¹, Sungho Nam^{1,2}, Hwajeong Kim^{1,3}, Thomas D Anthopoulos², Donal DC Bradley^{2,4} and Youngkyoo Kim¹

Organic nonvolatile memory transistors, featuring low-voltage operation (≤ 5 V) and high retention characteristics ($> 10\,000$ cycles), are demonstrated by introducing high molecular weight poly(vinyl alcohol) (PVA) as a gate insulating layer. PVA polymers with four different molecular weights (9.5–166 kDa) are examined for organic memory devices with poly(3-hexylthiophene) channel layers. All devices show excellent p-type transistor behavior and strong hysteresis in the transfer curves, but the lower molecular weight PVA delivers the higher hole mobility and the wider memory window. This has been attributed to the higher ratio of hydroxyl group dipoles that align in the out-of-plane direction of the PVA layers, as supported by impedance spectroscopy (dielectric constants), polarized Fourier transform-infrared spectroscopy and synchrotron radiation grazing incidence X-ray diffraction measurements. However, outstanding retention characteristics ($< 4\%$ current variation after 10 000 cycles) have been achieved with the higher molecular weight PVA (166 kDa) rather than the lower molecular weight PVA (9.5 kDa).

NPG Asia Materials (2016) 8, e235; doi:10.1038/am.2015.135; published online 15 January 2016

INTRODUCTION

Organic memory devices (OMDs) have attracted keen interest because of their advantages over conventional inorganic memory devices in that low-cost flexible plastic memory modules can be manufactured by employing large-area roll-to-roll coating processes.^{1–5} Achieving flexible plastic memory modules based on OMDs is of critical importance for the fabrication of real flexible electronic systems because inorganic semiconductors have a fundamental limitation in terms of flexibility owing to their rigid crystal structures.^{6–8} In addition, the performance of OMDs can be tailored by applying various types of organic semiconductors, which are manufactured via organic synthesis and modification/blend processes.^{9,10}

To date, two types of OMDs—resistor-type OMDs (ROMDs) and transistor-type OMDs (TOMDs)—have been most widely studied because of their potential for easy fabrication processes, leading to low-cost manufacturing of memory modules. The ROMDs have a diode structure with two electrodes, whereas three electrodes are typically used for the TOMDs. In the ROMDs, memory functions generally rely on charge transport and/or physical leakage paths.^{11–15} In particular, the ROMDs need additional transistor components for

active driving (addressing) of more than several millions of memory cells in memory modules, which inevitably gives rise to cost increases.^{16,17} In contrast, the TOMDs already possess their own transistors for active driving, so they are considered one of the simplest and most cost-effective memory devices for flexible plastic memory modules in the coming flexible electronics era.^{18,19}

It has been reported that TOMDs have memory functions from ferroelectric polymers, metal nanoparticles or charge trapping layers, and polymer energy well structures.^{20–30} However, most TOMDs reported to date have limitations with respect to high operation voltages and/or poor retention (stability) characteristics, even though basic memory functions in transistor structures can be well-demonstrated. Thus, it is very important to achieve both low voltage and high retention characteristics at the same time for further consideration toward commercialization of TOMDs, particularly for mobile applications, of which the first priority is low power consumption, as well as stability. Of various organic materials, poly(vinyl alcohol) (PVA) has also been introduced as a gate insulating layer for organic field-effect transistors to investigate a memory effect at high voltage (~ 80 V) (n-type small molecule),³¹ a hysteresis trend

¹Organic Nanoelectronics Laboratory, Department of Chemical Engineering, School of Applied Chemical Engineering, Kyungpook National University, Daegu, Republic of Korea; ²Center for Plastics Electronics, Department of Physics, Blackett Laboratory, Imperial College London, London, UK; ³Priority Research Center, Research Institute of Advanced Energy Technology, Kyungpook National University, Daegu, Republic of Korea and ⁴Department of Engineering Science and Physics, Division of Mathematical, Physical and Life Sciences, University of Oxford, Oxford, UK

Correspondence: Professor Y Kim, Organic Nanoelectronics Laboratory, Department of Chemical Engineering, School of Applied Chemical Engineering, Kyungpook National University, University Road 80, Daegu 702-701, Republic of Korea.
E-mail: ykimm@knu.ac.kr or khj217@knu.ac.kr

Received 12 August 2015; revised 4 October 2015; accepted 21 October 2015

(no memory study, p-type small molecule),³² and a typical transistor performance (no hysteresis/memory effect).^{33–35} However, no study has been reported on the influence of PVA molecular weights on the low-voltage operation and high retention stability of TOMDs with conjugated polymer channel layers.

In this work, we report the achievement of both low operation voltage (≤ -5 V) and long retention ($<4\%$ after 10 000 cycles) characteristics by employing high molecular weight PVA gate insulating layers in the TOMDs with poly(3-hexylthiophene) (P3HT) channel layers. The detailed effect of PVA molecular weight was investigated using PVA polymers with four weight-average molecular weights (9.5, 40.5, 93.5 and 166 kDa). The trend of the device performance with respect to the molecular weight was studied using various analysis/measurement techniques, such as atomic force microscopy (AFM), auger electron microscopy (AEM), polarized Fourier transform-infrared spectroscopy (FT-IR) and synchrotron radiation grazing incidence X-ray diffraction (GIXD).

MATERIALS AND METHODS

Materials and device fabrication

PVA with four weight-average molecular weights (9.5, 40.5, 93.5 and 166.0 kDa) was purchased from Sigma-Aldrich (St Louis, MO, USA), and P3HT (weight-average molecular weight = 30 kDa, polydispersity index = 1.7, regioregularity > 97%) was supplied by Rieke Metals (Lincoln, NE, USA).^{36,37} Prior to device fabrication, indium-tin oxide (ITO)-coated glass substrates were patterned to make 1×12 mm ITO stripes (as a gate electrode) via photolithography/etching. The patterned ITO-glass substrates were subjected to wet cleaning with acetone and isopropyl alcohol, followed by ultraviolet-ozone treatment at 28 mW cm^{-2} for 20 min. The PVA powder was dissolved in

deionized water at a solid concentration of $40\text{--}70 \text{ mg ml}^{-1}$ (9.5–166 kDa), while the P3HT solution was prepared using toluene at a solid concentration of 10 mg ml^{-1} . These solutions were stirred vigorously on a hot plate before spin-coating process. Then, the PVA layers (thickness = 250 nm) were spin-coated on the ITO-glass substrates and soft-baked at 70°C for 12 h. The P3HT layers (thickness = 60 nm) were subsequently spin-coated onto the PVA layers, followed by soft-baking at 60°C for 15 min. Finally, source/drain electrodes, Ni (10 nm) and Al (40 nm), were deposited on the P3HT layers through a shadow mask, defining the channel length of $70 \mu\text{m}$ and the channel width of 3 mm. All devices were stored in a nitrogen-filled glove box before measurements. The PVA layers (thickness = 250 nm) were spin-coated on the patterned ITO-glass substrates for spectroscopy and nanostructure measurements. For the measurement of dielectric constant, Al electrodes were deposited on top of the PVA layers coated on the ITO-glass substrates in a manner similar to that used for the transistor fabrication, which yielded a parallel plate-type glass/ITO/PVA/Al.

Measurements

Optical absorption spectra of the PVA layers coated on the ITO-glass substrates were measured using an ultraviolet–visible absorption spectrometer (Optizen 2120UV, Mecasys, Daejeon, South Korea). The thicknesses of the layers were measured using a surface profiler (Alpha Step 200, Tencor, Milpitas, CA, USA). The transistor and memory characteristics of the devices were measured using a semiconductor parameter analyzer (Keithley 4200, Keithley 2636B, Keithley Instruments, USA). An impedance analyzer (VersaSTAT 4, Princeton Applied Research, USA) was used to measure the dielectric constants of ITO/PVA/Al devices by a frequency sweep of up to 1 MHz. All devices were measured under inert conditions by employing a sample holder charged with argon gas. The nanostructure of the PVA layers was measured using a synchrotron radiation GIXD (wavelength = 1.212969 \AA , Pohang Accelerator Laboratory, Pohang, South Korea) and an AFM (Nanoscope IIIa, Digital Instruments, Billerica, MA, USA). The atom (oxygen) distribution in the PVA layers was analyzed with an AEM (PHI 700, ULVAC-PHI, Kanagawa, Japan). The cross-sectional areas of the devices were measured using a field-emission scanning electron microscope (FESEM, S-4800, Hitachi, Tokyo, Japan). The orientation of hydroxyl groups in the PVA layers (without any electric field) was measured with a FT-IR (5700 & Continuum, Thermo Scientific, Waltham, MA, USA).

RESULTS AND DISCUSSION

Figure 1a shows the device structure of the TOMDs with the PVA gate insulating layers (hereafter, abbreviated as PVA-TOMDs). Patterned ITO layers coated on glass substrates were used as a gate electrode, while source/drain electrodes were formed with Ni (thickness = 10 nm) and Al (thickness = 40 nm). The length and width of the channels were $70 \mu\text{m}$ and 3 mm, respectively. The thickness of all PVA layers was controlled to be 250 nm. As shown in Figure 1b, all PVA layers (thickness = 250 nm), which were coated on the ITO-glass substrates, were optically transparent, irrespective of their molecular weight (see the enlarged top-view photograph in Supplementary Figure S1). The SEM image disclosed that the 250-nm-thick PVA layer was well-formed and that a discrete interface was made with the P3HT layer after spin-coating (see Figure 1c).

The fabricated PVA-TOMDs were first subjected to an output test by sweeping drain voltage (V_D) at a fixed gate voltage (V_G). As shown in Figure 2, all devices exhibited p-type transistor behaviors with clear drain current (I_D) saturation in the output curves at low voltages ($V_D < -5$ V). This suggests that the PVA layers act properly as a gate insulator, irrespective of their molecular weight. Interestingly, the degree of hysteresis became larger at higher $|V_G|$, irrespective of PVA molecular weight, even though the sweep (forward and backward) range of V_D was the same for all devices. This result reflects that the hysteresis is more sensitive to V_G than V_D , which is indicative of gate-controlled hysteresis. In particular, the higher the PVA molecular weight, the lower the I_D value under the same voltage condition

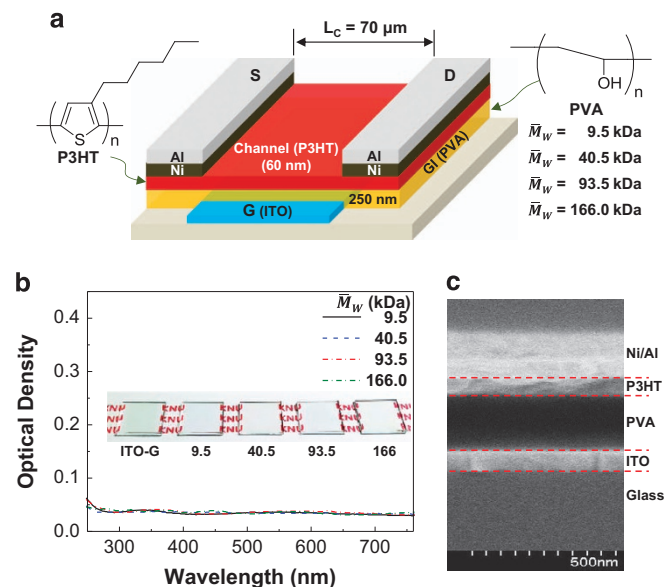


Figure 1 (a) Device structure for the organic memory transistor (PVA-TOMD) with the P3HT channel layer and the PVA memory gate insulating layer (see the weight-average molecular weights of PVA): ‘S’, ‘D’ and ‘G’ denote source, drain and gate electrodes, respectively. (b) Optical absorption spectra of the PVA layers (250 nm) coated on ITO-glass substrates according to the PVA molecular weight (inset: photograph of each sample). (c) Cross-sectional device structure of PVA-TOMD with the 250-nm-thick PVA layer and the 60-nm-thick P3HT layer (note that the thickness of each layer seems to be slightly deviated from the actual value, owing to the tilted state of the sample in the SEM measurement). ITO, indium-tin oxide; PVA-TOMD, poly(vinyl alcohol)-transistor-type organic memory device; SEM, scanning electron microscope.

($I_D = -760$ nA for 9.5 kDa and $I_D = -46.8$ nA for 166 kDa at $V_G = V_D = -5$ V). Thus, it is concluded that the performance of PVA-TOMDs is strongly affected by PVA molecular weight.

Next, transfer characteristics were examined for all PVA-TOMDs by sweeping V_G at a fixed V_D . As shown in Figure 3, I_D was gradually increased as V_G increased (negatively) up to -5 V at a fixed V_D (-1 V

and -3 V) in the forward sweep, irrespective of PVA molecular weight (note that the ON/OFF ratio ($I_{D,ON}/I_{D,OFF}$) was of the order of 10^4 – 10^5). However, the drain current in the backward sweep (from $V_G = -5$ V to $V_G = +5$ V) was significantly higher than that in the forward sweep (from $V_G = +5$ V to $V_G = -5$ V), even at lower V_D (-1 V) for all devices (see Supplementary Figure S2 for the direct comparison between the highest and lowest molecular weights). This result indicates that the PVA layers lead to a pronounced hysteresis in the present transistor structure, irrespective of their molecular weight. A close examination of the transfer curves shows that the maximum I_D values at $V_G = -5$ V are relatively higher for lower molecular weight than for higher molecular weight, which is in agreement with the output curves in Figure 2.

From the transfer curves in Figure 3, the hole mobility (μ_h) was calculated using $I_D = \frac{W}{2L}\mu_h C_i [(V_G - V_{TH})^2]$ in a saturation regime

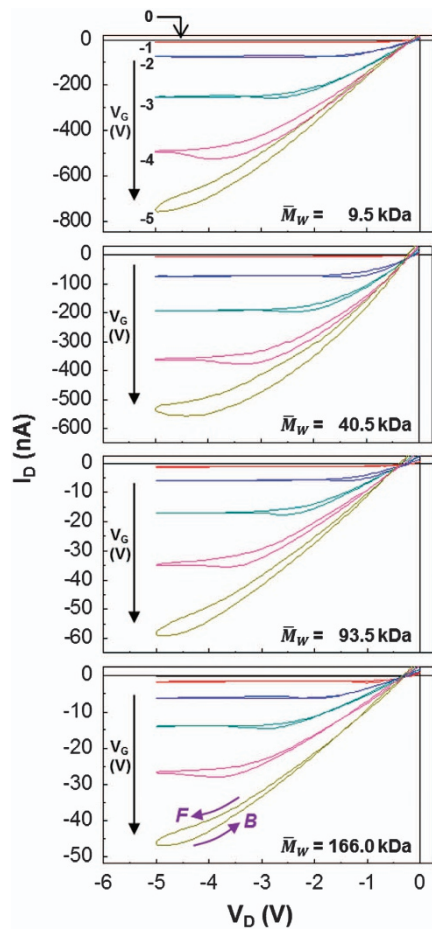


Figure 2 Output characteristics of the PVA-TOMDs according to the PVA molecular weight. 'F' and 'B' represent the forward (from 0 to -5 V) and backward (from -5 to 0 V) sweeps, respectively. The arrows denote the direction of the V_G increase (negatively) from 0 to -5 V by -1 -V steps. PVA-TOMD, poly(vinyl alcohol)-transistor-type organic memory device.

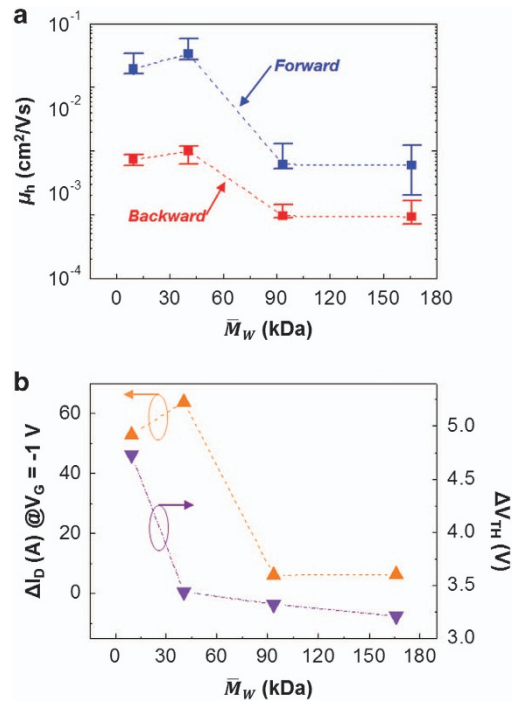


Figure 4 (a) Hole mobility (μ_h) of the PVA-TOMDs as a function of PVA molecular weight. (b) Drain current difference (ΔI_D) at $V_G = -1$ V and the threshold voltage difference (ΔV_{TH}) as a function of PVA molecular weight. PVA-TOMD, poly(vinyl alcohol)-transistor-type organic memory device.

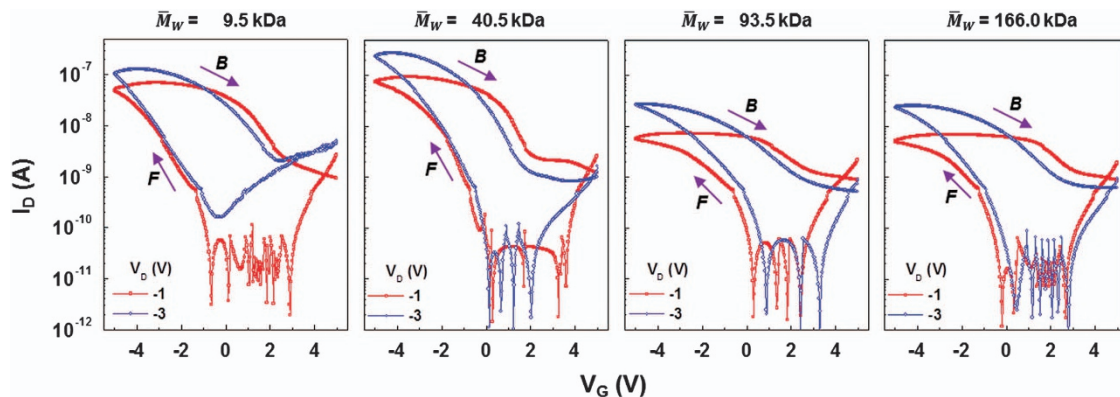


Figure 3 Transfer characteristics of the PVA-TOMDs according to the PVA molecular weight. 'F' and 'B' represent the forward (from $+5$ to -5 V) and backward (from -5 to $+5$ V) sweeps, respectively. PVA-TOMD, poly(vinyl alcohol)-transistor-type organic memory device.

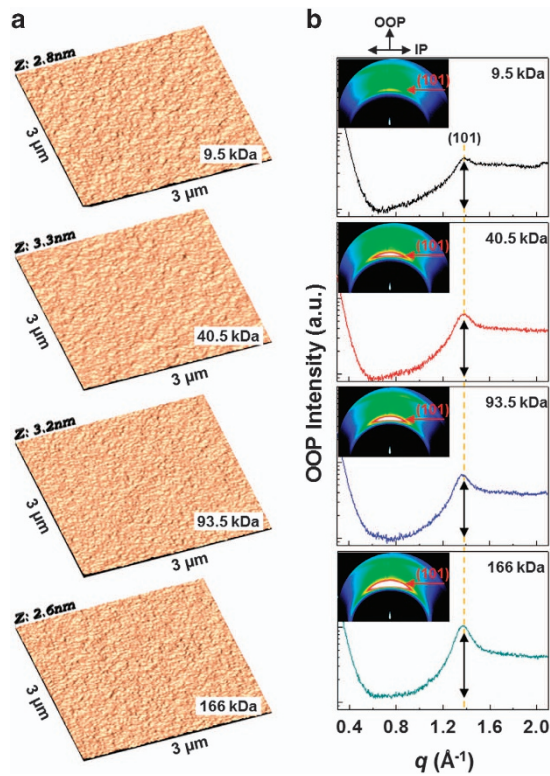


Figure 5 (a) Three-dimensional (3D) AFM images and (b) 1D GIXD profiles in the OOP direction (inset: 2D GIXD images) of the PVA films coated on the ITO-glass substrates. The PVA molecular weights are given on each graph. The double-sided arrows in the 1D GIXD profiles display the relative heights of (101) peaks. AFM, atomic force microscopy; GIXD, grazing incidence X-ray diffraction; OOP, out-of-plane; PVA, poly(vinyl alcohol).

($|V_G - V_{TH}| < |V_{DI}|$), where L , W and C_i are the channel length, the channel width and the capacitance of the gate insulator, respectively. As plotted in Figure 4a, higher hole mobility was obtained for the devices with lower molecular weight PVA, irrespective of the sweep direction. This supports the fact that a higher I_D was measured for the lower molecular weight PVA in the output and transfer curves (see Figures 2 and 3). Here, the relatively lower hole mobility in the backward sweep compared with that in the forward sweep can be attributed to retarded hole transport, owing to the holes charged in the forward sweep. This may be one of the reasons why remarkable hysteresis was achieved in the present PVA-TOMDs. As shown in Figure 4b, the differences in I_D ($V_G = -1$ V) and threshold voltage (V_{TH}) between the forward and backward sweeps were relatively higher for the lower molecular weight PVA, which indicates that a better memory window can be achieved for the lower molecular weight PVA (see Supplementary Table S1).

To understand the different performances of PVA-TOMDs with respect to the PVA molecular weight, the nanostructure of the PVA layers was examined using AFM, AEM and GIXD measurements. As shown in Figure 5a, no particular surface nanostructures were measured for the PVA layers, irrespective of PVA molecular weight, in the presence of very slight surface (root-mean-square) roughness variation from 0.36 nm (9.5 kDa) to 0.32 nm (166 kDa). In addition, hydroxyl groups in the PVA layers were found to randomly distribute without peculiar aggregations, irrespective of molecular weight, as evidenced from the AEM images (see Supplementary Figure S3). However, as observed in the two-dimensional GIXD images in

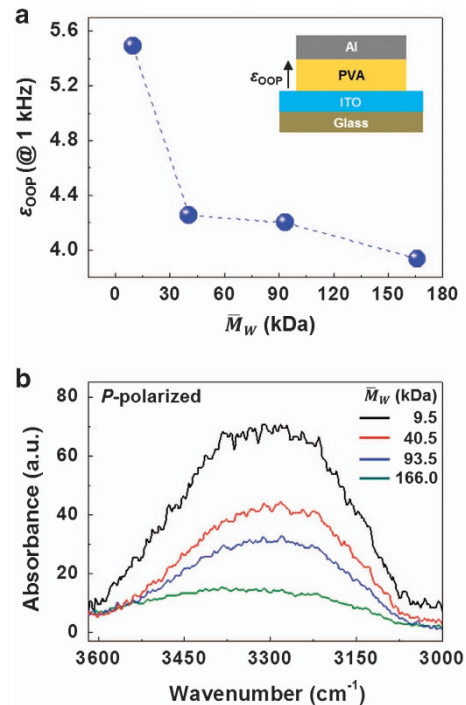


Figure 6 (a) Dielectric constant (ϵ_{OOP}) of the PVA layers as a function of PVA molecular weight: the measurement was carried out with a simple device structure (inset) at a frequency of 1 kHz. (b) P-polarized FT-IR absorption spectra of the PVA layers, which were coated on ITO-glass substrates, according to the PVA molecular weight. FT-IR, Fourier transform-infrared spectroscopy; PVA, poly(vinyl alcohol).

Figure 5b (inset), the Debye ring intensity for the (101) diffraction was higher for the PVA layer with the higher molecular weight.^{38,39} This result means that a higher degree of crystallinity is made for the PVA layer with the higher molecular weight (see one-dimensional GIXD profiles in Figure 5 and Supplementary Figure S4). The huge anisotropy in the (101) intensity between the out-of-plane (OOP) and in-plane (IP) directions discloses that the PVA chain stacking leading to the (101) crystal plane did preferentially occur in the OOP direction, irrespective of the PVA molecular weight. In addition, we find that higher anisotropy in the degree of crystallinity between the OOP and the IP directions was achieved for the PVA layer with the higher molecular weight (see Supplementary Figure S4). Considering the PVA chain stacking in the crystal structure, the orientation of the hydroxyl (OH) groups in the IP direction may be more preferred for the PVA layer with the higher molecular weight. This preferential orientation of hydroxyl groups in the IP direction may be one of the clues as to why the performance (drain current) of the transistors was poor in the case of higher molecular weight PVA (see Figures 2 and 3). The direction of the hydroxyl groups greatly influences the polarizability (dielectric constant) in the OOP (thickness) direction of the PVA layers, which is of critical importance in the gate-control operation of transistors.

To validate the change in the dielectric constant according to the PVA molecular weight, a simple parallel plate-type device was fabricated by sandwiching the PVA layers between two electrodes (see inset in Figure 6a). The measurement result showed that the dielectric constant in the OOP direction was indeed higher for the PVA layers with the lower molecular weights (see Figure 6a). This result is further supported by the polarized FT-IR measurement that disclosed more hydroxyl groups oriented in the OOP direction for the

PVA layer with the lower molecular weight (see Figure 6b). The ratios of hydroxyl groups oriented in the OOP direction to all hydroxyl groups were 52% (9.5 kDa), 24% (40.5 kDa), 17% (93.5 kDa) and 7% (166 kDa). Hence, it can be concluded that the PVA molecular weight strongly affects the performance of PVA-TOMDs due to the orientations of hydroxyl groups, as illustrated in Figure 7.

Finally, the present PVA-TOMDs were subjected to the memory function test to determine which molecular weight is the best for durable memory devices. As shown in Figure 8, stable write-once-reading-many (WORM) operations were successfully performed for all devices, irrespective of the molecular weight (see the enlarged plots in Supplementary Figure S5). This result indicates that all of the present devices actually function as a nonvolatile memory. Here, it is worthy

to note that the drain current level was relatively lower for the higher molecular weight PVA, which may be helpful with regard to the realization of low-power plastic memory devices. Next, the retention performances of the same PVA-TOMDs were examined by applying the continuous full-cycle operation of writing–reading–erasing–reading (WRER) at room temperature. Interestingly, relatively unstable memory characteristics in the WR operation were measured for the device with the low molecular weight (9.5 kDa) PVA layer (see Figure 9 and Supplementary Figure S6). However, the PVA-TOMD with the high molecular weight (166 kDa) PVA layer exhibited extremely stable memory performances, even after 10 000 cycles

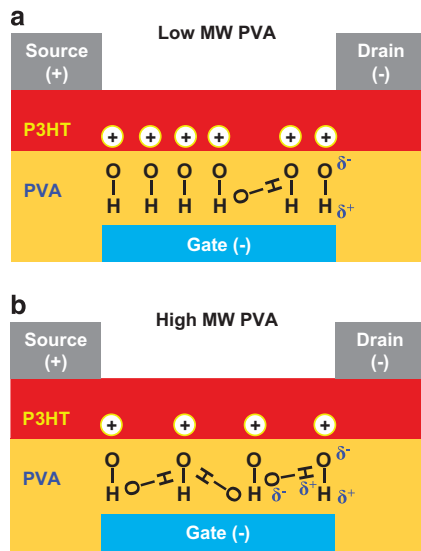


Figure 7 Illustration for the proposed orientation of the hydroxyl (OH) groups in the PVA layers of PVA-TOMDs on operation ($V_G < 0$ V and $V_D < 0$ V): (a) low molecular weight PVA and (b) high molecular weight PVA. Note that the positive charges (see the circled '+' symbols) can be generated by the negative ends of the OH dipoles that are oriented in the OOP direction of the film plane. OOP, out-of-plane; PVA-TOMD, poly(vinyl alcohol)-transistor-type organic memory device.

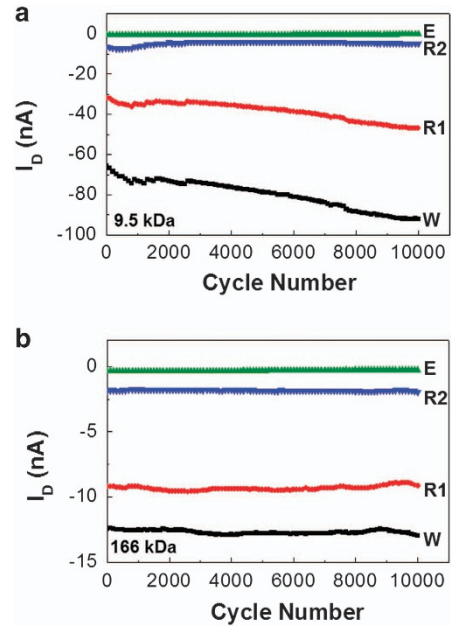


Figure 9 Retention characteristics for the PVA-TOMDs (a: 9.5 kDa, b: 166 kDa) by applying continuous writing–reading–erasing–reading (WRER) cycles: W (writing at $V_G = -5$ V) → R1 (reading at $V_G = -1$ V) → E (erasing at $V_G = +5$ V) → R2 (reading at $V_G = -1$ V). Note that the drain voltage was fixed at $V_D = -2$ V for the entire measurement (10 000 cycles). PVA-TOMD, poly(vinyl alcohol)-transistor-type organic memory device.

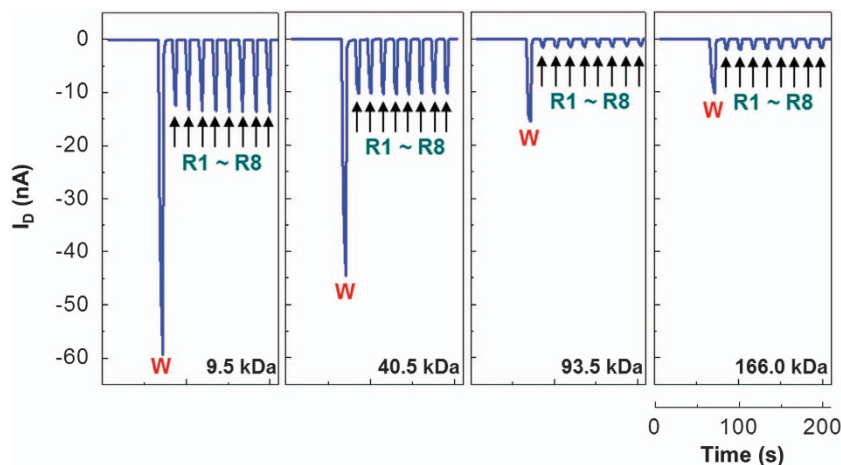


Figure 8 Writing-once-reading-many (WORM) operations for the PVA-TOMDs according to the PVA molecular weight. The writing (W) operation was performed at $V_G = -5$ V and $V_D = -2$ V, whereas the reading (R1–R8) operation was performed at $V_G = -1$ V and $V_D = -2$ V. PVA-TOMD, poly(vinyl alcohol)-transistor-type organic memory device.

(WRER). The change in the drain current level was only 4.2% for writing (W) at $V_G = -5$ V and 0.2% for reading high (R1) at $V_G = -1$ V, whereas the average variation for all WRER events was <4%, even after 10 000 cycles. In addition, the retention time test also disclosed that better stability could be achieved for the PVA with the higher molecular weight (see Supplementary Figure S7). Therefore, it is concluded that the high molecular weight PVA is better for durable memory devices due to its excellent retention characteristics, as well as its low power consumption, whereas the low molecular weight PVA is suitable for switching applications with regard to the high current level.

CONCLUSION

TOMDs were fabricated by employing the PVA layers as a memory gate insulator with four different molecular weights. All devices exhibited excellent output performances with clear current saturation at low voltages ($|V_G| \leq 5$ V), while typical transfer curves were measured in the forward sweep (ON/OFF ratio up to $\sim 10^5$). Interestingly, higher drain current was measured for the lower molecular weight PVA, leading to a higher hole mobility for the lower molecular weight PVA. In particular, strong hysteresis in the drain current was measured from the transfer curves. This was even more pronounced for all molecular weights in the presence of a better memory window for the lower molecular weight PVA. The better performances (hole mobility and memory window) for the lower molecular weight PVA were attributed to the higher orientation ratio of the hydroxyl group dipoles in the thickness (OOP) direction of the PVA layer. However, better retention characteristics were measured for the higher molecular weight PVA (<4% variation after 10 000 cycles). Hence, it is expected that the commercialization of plastic memory modules can be positively considered because both low-voltage operation and stable retention characteristics are achieved for the present PVA-TOMDs with the high molecular weight (166 kDa) PVA gate insulator. Finally, the present memory transistors are expected to contribute to the viable manufacturing of flexible organic memory module devices by utilizing solution-processes of core layers at low (room) temperatures.

CONFLICT OF INTEREST

The authors declare no conflict of interest.

ACKNOWLEDGEMENTS

This work was financially supported by grants from Korean Government (Basic Research Laboratory Program_2011-0020264, Basic Science Research Program_2009-0093819, NRF_2015R1A2A2A01003743, MOTIE_10048434, NRF_2014R1A1A3051165, Human Resource Training Project for Regional Innovation_MOE(NRF_2014H1C1A1066748) and NRF_2014H1A2A1016454). We thank Dr Boknam Chae and Prof Seung Woo Lee for their help with the IR measurements.

- Scott, J. C. & Bozano, L. D. Nonvolatile memory elements based on organic materials. *Adv. Mater.* **19**, 1452–1463 (2007).
- Naber, R. C. G., Asadi, K., Blom, P. W. M., de Leeuw, D. M. & de Boer, B. Organic nonvolatile memory devices based on ferroelectricity. *Adv. Mater.* **22**, 933–945 (2010).
- Ling, Q.-D., Liaw, D.-J., Zhu, C., Chan, D. S.-H., Kang, E.-T. & Neoh, K.-G. Polymer electronic memories: materials, devices and mechanisms. *Prog. Polym. Sci.* **33**, 917–978 (2008).
- Heremans, P., Gelinck, G. H., Müller, R., Baeg, K.-J., Kim, D.-Y. & Noh, Y.-Y. Polymer and organic nonvolatile memory devices. *Chem. Mater.* **23**, 341–358 (2011).
- Nam, S., Kim, J., Lee, H., Kim, H., Ha, C.-S. & Kim, Y. Doping effect of organosulfonic acid in poly(3-hexylthiophene) films for organic field-effect transistors. *ACS Appl. Mater. Interfaces* **4**, 1281–1288 (2012).

- Sun, Y. & Rogers, J. A. Inorganic semiconductors for flexible electronics. *Adv. Mater.* **19**, 1897–1916 (2007).
- Forrest, S. R. The path to ubiquitous and low-cost organic electronic appliances on plastic. *Nature* **428**, 911–918 (2004).
- Lewis, J. Material challenge for flexible organic devices. *Mater. Today* **9**, 38–45 (2006).
- Cheng, Y.-J., Yang, S.-H. & Hsu, C.-S. Synthesis of conjugated polymers for organic solar cell applications. *Chem. Rev.* **109**, 5868–5923 (2009).
- Dailey, S., Feast, W. J., Peace, R. J., Sage, I. C., Till, S. & Wood, E. L. Synthesis and device characterisation of side-chain polymer electron transport materials for organic semiconductor applications. *J. Mater. Chem.* **11**, 2238–2243 (2001).
- Gao, S., Song, C., Chen, C., Zeng, F. & Pan, F. Dynamic processes of resistive switching in metallic filament-based organic memory devices. *J. Phys. Chem. C* **116**, 17955–17959 (2012).
- Casula, G., Cosseddu, P., Busby, Y., Pireaux, J.-J., Rosowski, M., Szczesna, B. T., Soliwoda, K., Celi-chowski, G., Grobelny, J., Novák, J., Banerjee, R., Schreiber, F. & Bonfiglio, A. Air-stable, non-volatile resistive memory based on hybrid organic/inorganic nanocomposites. *Org. Electron.* **18**, 17–23 (2015).
- Hu, B., Wang, C., Wang, J., Gao, J., Wang, K., Wu, J., Zhang, G., Cheng, W., Venkateswarlu, B., Wang, M., Lee, P. S. & Zhang, Q. Inorganic-organic hybrid polymer with multiple redox for high-density data storage. *Chem. Sci.* **5**, 3404–3408 (2014).
- Tan, C., Liu, Z., Huang, W. & Zhang, H. Non-volatile resistive memory devices based on solution-processed ultrathin two-dimensional nanomaterials. *Chem. Soc. Rev.* **44**, 2615–2628 (2015).
- Asadi, K., de Leeuw, D. M., de Boer, B. & Blom, P. W. M. Organic non-volatile memories from ferroelectric phase-separated blends. *Nat. Mater.* **7**, 547–550 (2008).
- Nam, S., Ko, Y.-G., Hahn, S., Park, S., Seo, J., Lee, H., Kim, H., Reo, M. & Kim, Y. Organic nonvolatile memory transistors with self-doped polymer energy well structures. *NPG Asia Mater.* **5**, e33 (2013).
- Sekitani, T., Yokota, T., Zschieschang, U., Klauk, H., Bauer, S., Takeuchi, K., Takamiya, M., Sakurai, T. & Someya, T. Organic nonvolatile memory transistors for flexible sensor arrays. *Science* **326**, 1516–1519 (2009).
- Egginger, M., Bauer, S., Schwödiouer, R., Neugebauer, H. & Sariciftci, N. S. Current versus gate voltage hysteresis in organic field effect transistors. *Monatsh. Chem.* **140**, 735–750 (2009).
- Leong, W. L., Mathews, N., Tan, B., Vaidyanathan, S., Dötz, F. & Mhaisalkar, S. Towards printable organic thin film transistor based flash memory devices. *J. Mater. Chem.* **21**, 5203–5214 (2011).
- Wang, W., Hwang, S. K., Kim, K. L., Lee, J. H., Cho, S. M. & Park, C. Highly reliable top-gated thin-film transistor memory with semiconducting, tunneling, charge-trapping, and blocking layers all of flexible polymers. *ACS Appl. Mater. Interfaces* **7**, 10957–10965 (2015).
- Chang, M.-F., Lee, P.-T., McAlister, S. P. & Chin, A. A flexible organic pentacene nonvolatile memory based on high- κ dielectric layers. *Appl. Phys. Lett.* **93**, 233302 (2008).
- Kim, S.-J., Park, Y.-S., Lyu, S.-H. & Lee, J.-S. Nonvolatile nano-floating gate memory devices based on pentacene semiconductors and organic tunneling insulator layers. *Appl. Phys. Lett.* **96**, 033302 (2010).
- Naber, R. C. G., Tanase, C., Blom, P. W. M., Gelinck, G. H., Marsman, A. W., Touwslager, F. J., Setayesh, S. & de Leeuw, D. M. High-performance solution-processed polymer ferroelectric field-effect transistors. *Nat. Mater.* **4**, 243–248 (2005).
- Lee, K. H., Lee, G., Lee, K., Oh, M. & Im, S. Flexible low voltage nonvolatile memory transistors with pentacene channel and ferroelectric polymer. *Appl. Phys. Lett.* **94**, 093304 (2009).
- Schroeder, R., Majewski, L. A., Voigt, M. & Grell, M. Memory performance and retention of an all-organic ferroelectric-like memory transistor. *IEEE Electron Device Lett.* **26**, 69–71 (2005).
- Baeg, K.-J., Kim, D., Kim, J., Yang, B.-D., Kang, M., Jung, S.-W., You, I.-K., Kim, D.-Y. & Noh, Y.-Y. High-performance top-gated organic field-effect transistor memory using electrets for monolithic printed flexible NAND flash memory. *Adv. Funct. Mater.* **22**, 2915–2926 (2012).
- Kim, T.-W., Gao, Y., Acton, O., Yip, H.-L., Ma, H., Chen, H. & Jen, A. K.-Y. Graphene oxide nanosheets based organic field effect transistor for nonvolatile-memory applications. *Appl. Phys. Lett.* **97**, 023310 (2010).
- Stadler, P., Oppelt, K., Singh, T. B., Grote, J. G., Schwödiouer, R., Bauer, S., Pigmayer-Brezina, H., Bäuerle, D. & Sariciftci, N. S. Organic field-effect transistors and memory elements using deoxyribonucleic acid (DNA) gate dielectric. *Org. Electron.* **8**, 648–654 (2007).
- Lee, J. H., Yew, S. C., Cho, J. & Kim, Y. S. Effect of redox proteins on the behavior of non-volatile memory. *Chem. Commun.* **48**, 12008–12010 (2012).
- Tsai, T.-D., Chang, J.-W., Wen, T.-C. & Guo, T.-F. Manipulating the hysteresis in poly(vinyl alcohol)-dielectric organic field-effect transistors toward memory elements. *Adv. Funct. Mater.* **23**, 4206–4214 (2013).
- Singh, Th. B., Marjanović, N., Matt, G. J., Sariciftci, N. S., Schwödiouer, R. & Bauer, S. Nonvolatile organic field-effect transistor memory element with a polymeric gate electret. *Appl. Phys. Lett.* **85**, 5409–5411 (2004).
- Wang, W., Ma, D., Pan, S. & Yang, Y. Hysteresis mechanism in low-voltage and high mobility pentacene thin-film transistors with polyvinyl alcohol dielectric. *Appl. Phys. Lett.* **101**, 033303 (2012).
- Jang, Y., Kim, D. H., Park, Y. D., Cho, J. H., Hwang, M. & Cho, K. Low-voltage and high-field-effect mobility organic transistors with a polymer insulator. *Appl. Phys. Lett.* **88**, 072101 (2006).

- 34 Machado, W. S. & Hümmelgen, I. A. Low-voltage poly(3-hexylthiophene)/poly(vinyl alcohol) field-effect transistor and inverter. *IEEE Trans. Electron Dev.* **59**, 1529–1533 (2012).
- 35 Rossi, L., Seidel, K. F., Machado, W. S. & Hümmelgen, I. A. Low voltage vertical organic field-effect transistor with polyvinyl alcohol as gate insulator. *J. Appl. Phys.* **110**, 094508 (2011).
- 36 Nam, S., Lee, S., Lee, I., Shin, M., Kim, H. & Kim, Y. Nanomorphology-driven two-stage hole mobility in blend films of regioregular and regiorandom polythiophenes. *Nanoscale* **3**, 4261–4269 (2011).
- 37 Seo, J., Park, S., Nam, S., Kim, H. & Kim, Y. Liquid crystal-on-organic field-effect transistor sensory devices for perceptive sensing of ultralow intensity gas flow touch. *Sci. Rep.* **3**, 2452 (2013).
- 38 Mohamad, A. A., Mohamed, N. S., Yahya, M. Z. A., Othman, R., Ramesh, S., Alias, Y. & Arof, A. K. Ionic conductivity studies of poly(vinyl alcohol) alkaline solid polymer electrolyte and its use in nickel–zinc cells. *Solid State Ionics* **156**, 171–177 (2003).
- 39 Assender, H. E. & Windle, A. H. Crystallinity in poly(vinyl alcohol). 1. An X-ray diffraction study of atactic PVOH. *Polymer* **39**, 4295–4302 (1998).



This work is licensed under a Creative Commons Attribution 4.0 International License. The images or other third party material in this article are included in the article's Creative Commons license, unless indicated otherwise in the credit line; if the material is not included under the Creative Commons license, users will need to obtain permission from the license holder to reproduce the material. To view a copy of this license, visit <http://creativecommons.org/licenses/by/4.0/>

Supplementary Information accompanies the paper on the NPG Asia Materials website (<http://www.nature.com/am>)